

Surface-enhanced Raman spectroscopic study of hydrogen and deuterium chemisorption on diamond (111) and (100) surfaces

Koichi Ushizawa, Mikka N.-Gamo, Yuko Kikuchi, Isao Sakaguchi, Yoichiro Sato, and Toshihiro Ando*
 Core Research for Evolutional Science and Technology (CREST) of Japan Science and Technology Corporation (JST),
 c/o National Institute for Research in Inorganic Materials (NIRIM), 1-1 Namiki, Tsukuba, Ibaraki 305-0044, Japan

(Received 6 April 1999)

Surface-enhanced Raman scattering spectroscopy has been applied so that hydrogen chemisorption on the diamond (111) and (100) surfaces could be observed. Raman scattering signals from the surface species were enhanced by means of contact with thin Ag films. C-H stretching vibrations were observed in the region 2800–3000 cm^{-1} from the hydrogenated diamond surface. C-D stretching vibrations were observed in the region 2050–2250 cm^{-1} from the deuterated diamond surface. C-H and C-D stretching vibration modes were assigned according to *ab initio* molecular orbital calculations. [S0163-1829(99)51032-1]

INTRODUCTION

Vibrational spectroscopy is one of the most powerful techniques for observing species that have been chemisorbed on diamond surfaces, and especially for observing hydrogen chemisorption. Hydrogen chemisorption on diamond has been the focus of many studies because of its role in stabilizing the surface, its vapor phase growth mechanisms, surface electric conductivity, negative electron affinity, and so on. Vibrational spectroscopy has the additional advantage of the isotope effect, which makes it possible to distinguish chemisorption from background physisorption. The isotopic shift of the vibrational frequencies can be estimated with a simple equation. Recently, many vibrational spectroscopic studies have been presented including the following three techniques: high resolution electron energy loss spectroscopy (HREELS),^{1–3} Fourier-transform infrared (FTIR),^{4–6} and sum frequency generation (SFG).^{7–9} However, no Raman spectroscopic study has been reported. Raman spectroscopy emerged mainly for its use in characterizing the bulk quality of diamond and carbons. Generally, Raman scattering sensitivity is not high enough to serve as a surface probe. However, strong enhancements of Raman scattering have been reported from use with adsorbates on Ag electrodes in solution. Several explanations have been given for the enhancement called surface-enhanced Raman scattering (SERS).^{10–14} SERS spectroscopy using micro-Raman optics has a great advantage for use with small crystals such as chemical vapor deposited (CVD) diamond crystals, *c*-BN, and other new materials, which would be difficult to obtain as large single crystals. Normally, other techniques (HREELS, FTIR) require significantly large sample size crystals, at least several mm in size. In contrast, laser micro-Raman spectroscopy can easily focus on a micrometer spot in the sample. In this paper, we present the results of applying SERS to hydrogen chemisorption on the diamond (111) and (100) surfaces. *Ab initio* molecular orbital calculations provide conclusive agreements to the vibrational frequencies obtained in these experiments.

EXPERIMENT

Natural and high-pressure high-temperature synthetic (HP-HT) diamond (111) and (100) were used as the substrate

crystals. The substrates were polished and cleaned with HCl, HNO₃ acid, then rinsed with distilled water. Hydrogenation was performed at 800 °C in hydrogen plasma generated by a 2.45-GHz microwave, conditions which are similar to those of CVD diamond growth. After the hydrogen-plasma treatment, the samples were transferred to a UHV chamber in order to observe low energy electron diffraction (LEED). Then, normal Raman and SERS experiments were performed. Chemical vapor deposited diamond crystals on Si substrate were also investigated by using SERS spectroscopy. The CVD crystals had a well-faceted cubo-octahedral shape and were about 10 μm in size. The crystal surfaces consisted of triangle (111) and square (100) facets.

Ag films were prepared by a vacuum evaporation technique at room temperature in a second vacuum chamber below the pressure of 1×10^{-7} Torr. The deposition rate of Ag was kept at approximately 0.05 nm s^{-1} by adjusting the filament current. The deposited Ag were island films with an average thickness of 15–20 nm.

Raman spectra were recorded using a laser Raman microprobe with confocal collection optics having a spatial resolution of approximately 1 μm . The single-mode 514.5-nm line of an Ar⁺ ion laser was used for excitation. Low laser power of 5 mW was employed on the sample surface so that no appreciable peak shift or peak broadening was caused by the irradiation heating. A liquid nitrogen cooled charge-coupled device (CCD) was used for the photon detection. The average exposure time was about 2 min, and 30 scans were accumulated for each spectrum.

AB INITIO CALCULATION

Ab initio self-consistent field (SCF) molecular orbital (MO) calculations were carried out using a GAUSSIAN 98 package.¹⁵ Figure 1 shows cluster models of the hydrogenated diamond surfaces. The C-C bond has the highest covalency feature and the clusters with only pure carbon atoms are unstable because of many dangling bonds. We used the cluster models terminated with hydrogen. The geometries of the cluster models were optimized at the restricted Hartree-Fock (HF) level with the 6–31+*G*(*d*,*p*) basis set. The force constant and frequencies were calculated at the optimized geometries. Cluster (a) of Fig. 1 consists of C₁₀H₁₅ and CH₃,

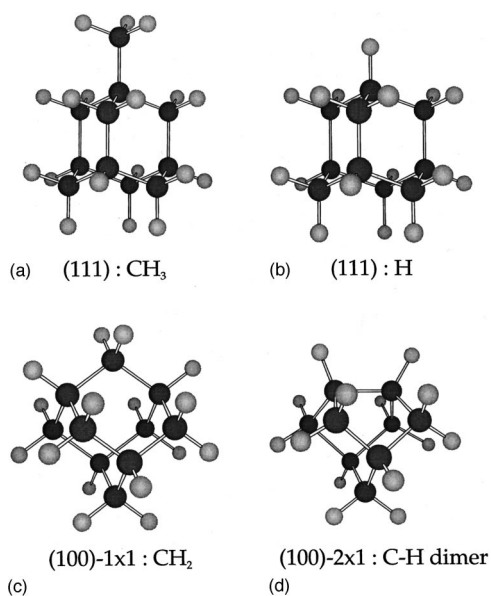


FIG. 1. Cluster models of hydrogenated and deuterated diamond for *ab initio* MO calculations. (a) C₁₀H₁₅+CH₃ cluster model for CH₃ chemisorption on the diamond (111) surface. (b) C₁₀H₁₅+H cluster model for C-H chemisorption on the diamond (111) surface. (c) C₉H₁₄+CH₂ cluster model for CH₂ chemisorption on the diamond (100)-1×1 surface. (d) C₉H₁₄, (C-H)₂ dimer cluster model for C-H chemisorption on the diamond (100)-2×1 surface.

which correspond to the diamond (111) surface covered with CH₃ groups. Cluster (b) of Fig. 1 consists of C₁₀H₁₅ and H, which correspond to the diamond (111) surface terminated with monohydride. Cluster (c) of Fig. 1 is equivalent to cluster (b). The CH₂ of the model corresponds to the surface of the diamond (100) terminated with dihydride. Cluster (d) of Fig. 1 corresponds to the dimer structure of the diamond (100)-2×1 terminated with monohydride. Vibrational frequencies of CH₃ groups were calculated for the CH₃ termination of the (111) surfaces by using cluster (a). Frequencies of CH₂ groups were calculated for the dihydride termination of the (100)-1×1 surfaces by using cluster (c). Frequencies of C-H were calculated for the monohydride termination of the (111) surfaces using cluster (b), and those for the monohydride termination of the (100)-2×1 surfaces by using cluster (d). It is well known that the HF level computation tends to estimate a 10–15% higher value because of the neglect of anharmonic effects.^{16,17} Scaling techniques are generally considered to correct them.^{16–18} In this study, the calculated frequencies are scaled uniformly by 0.9.

RESULTS

Raman scattering intensities from diamond surface species were strongly enhanced with the Ag films. Figure 2 shows Raman scattering from the hydrogenated and deuterated diamond (111) surfaces in the C-H and C-D stretching regions without Ag in the spectra (a) and (c), and with thin Ag film in the spectra (b) and (d). While almost no feature was observed without Ag in the spectra (a) and (c), peaks due to C-H stretching vibrations were clearly observed with

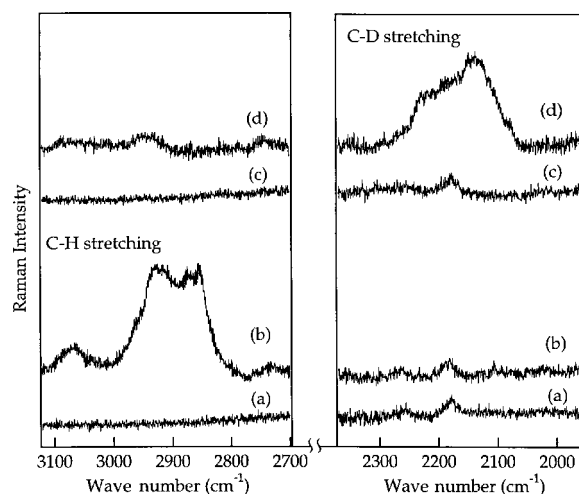


FIG. 2. Raman spectra from the hydrogenated and deuterated (111) surfaces. (a) Hydrogenated diamond (111) surface without Ag. (b) Hydrogenated diamond (111) surface with Ag, SERS. (c) Deuterated diamond (111) surface without Ag. (d) Deuterated diamond (111) surface with Ag, SERS.

Ag contact in the spectrum (b). A small peak observed around 2180 cm⁻¹ was assigned to be a portion of second-order Raman scattering of the bulk diamond crystal without Ag in the spectrum (c).¹⁹ On the other hand, significant large peaks were observed with thin Ag film in the region 2050–2250 cm⁻¹ due to C-D stretching vibrations in the spectrum (d). For the same sample, a very weak peaking due to C-H stretching vibrations was observed in the region 2800–3100 cm⁻¹. This very weak intensity was evaluated to be the background contamination level. Strong C-D peaks and very weak C-H peaks suggested that the contamination level was negligibly low in the spectrum (c). This result clearly indicated that Raman scattering intensities were strongly enhanced by the contact with thin Ag films. SERS with thin Ag film is generally considered useful for observing the surface species on diamond crystals.

Low energy electron diffraction (LEED) obtained from the hydrogenated diamond (111) indicated a 1×1 fundamental structure. LEED from the hydrogenated diamond (100) indicated a 2×1/1×2 reconstructed structure. These patterns were similar to those usually observed on the hydrogenated diamond surfaces. Figure 3(I) shows the spectral difference between the hydrogenated (111)-1×1 and the (100)-2×1 in the SERS. The spectrum observed from the triangle facet of the CVD well-faceted cubo-octahedral diamond crystals was similar to that shown in Fig. 3(a), and that obtained from the square facet was quite similar to that shown in Fig. 3(b). Figure 3(a) shows strong peaks due to C-H stretching vibrations of *sp*³ carbons from 2800–3000 cm⁻¹. A weak peak around 3000–3100 cm⁻¹ was due to C-H stretching vibrations of *sp*² carbons. A very weak peak observed at 2750 cm⁻¹ was not assigned. The main C-H stretching peaks could be decomposed into three parts: a medium peak at 2850 cm⁻¹, a medium peak at 2870 cm⁻¹, and a strong peak at 2925 cm⁻¹. Spectrum (b) of the (100)-2×1 surface shows a different feature from spectrum (a) of the (111)-1×1 surface. The main peaks in the 2800–3000 cm⁻¹ also could be decomposed into three parts: a weak peak at 2830

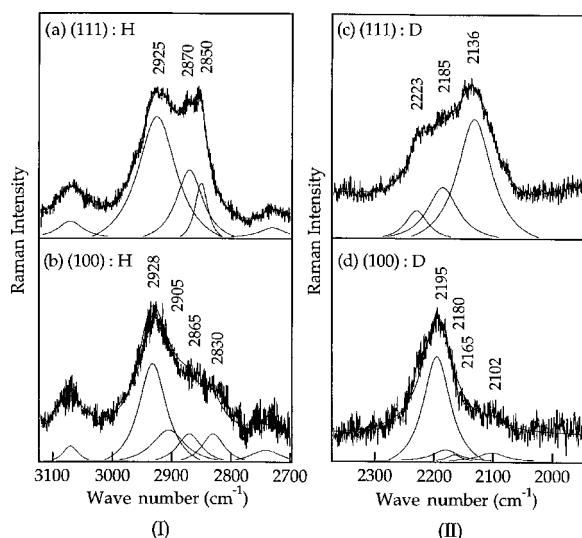


FIG. 3. SERS spectra from the diamond (111) and (100) surfaces. (I) Hydrogenated surfaces with Ag. (II) Deuterated surfaces with Ag. (a) Hydrogenated diamond (111) surface. (b) Hydrogenated diamond (100) surface. (c) Deuterated diamond (111) surface. (d) Deuterated diamond (100) surface.

cm^{-1} , a weak peak at 2865 cm^{-1} , and a strong peak at 2928 cm^{-1} .

Figure 3 (II) shows SERS spectra from the deuterated diamond (111) and (100). Peaks due to C-D stretching vibrations were observed in the region $2050\text{--}2250 \text{ cm}^{-1}$ in both spectra. The peaks consisted of three peaks: at 2136 , 2185 , and 2223 cm^{-1} , respectively, in the spectrum of the (111) surface. The peak feature of the C-D stretching was different from that of the C-H stretching on the diamond (111) surface. The main component of the C-D stretching vibrations was a peak at 2136 cm^{-1} . In contrast, the peak feature on the (100) surface was very similar to that between the C-H and C-D stretching vibrations.

DISCUSSION

Diamond (111)

The *ab initio* calculation was used to estimate the vibrational frequencies. The calculated values and the Raman spectra for the C-H stretching vibrations are shown in Figs. 4(a) and 4(b), and those for the C-D stretching vibrations are shown in Figs. 4(c) and 4(d). The C-H stretching vibrations on the diamond (111) consist of three modes: (i) CH_3 symmetric vibration mode at 2853 cm^{-1} ; (ii) CH_3 degenerate stretching vibration at 2905 cm^{-1} ; and (iii) C-H stretching vibration at 2868 cm^{-1} . These modes are in good agreement with the SERS experimental results. Table I summarizes the frequencies observed by the present SERS experiment and those presented in previous vibrational spectroscopic experiments compared with the present *ab initio* calculation results. Previous FTIR studies also support the present results. SERS peaks due to C-H and C-D species appeared in the same wave number region as FTIR peaks.⁴ However, reported FTIR studies cannot distinguish the crystal plane information because powder polycrystal diamond surfaces were used.

HREELS studies have revealed that the diamond (111) surface can be covered with CH_3 groups by the angular dependence of the vibrations.³ HREELS has less resolution to divide the C-H stretching peaks corresponding to each vibrational mode, though HREELS can distinguish the different vibration modes by different scattering mechanisms such as a long distance dipole field scattering or an impact scattering. The SERS spectrum suggested that the intensity of the CH_3 vibrations was much greater than that of C-H vibrations. This result indicates that a significant number of CH_3 groups conclusively exist on the hydrogenated diamond (111) surfaces.

Diamond (100)- 2×1

As LEED suggested, the hydrogenated diamond (100) surface has been reconstructed to 2×1 periodicity. HREELS

TABLE I. Assignment of C-H chemisorbed species on the diamond surfaces.

Mode ^a / cm^{-1}	CH str.				(111) surface	(100) surface	References
	CH_3 sym. str.	CH_3 deg. str.	CH_2 sym. str.	CH_2 asym. str.			
SERS(111)	2850	2925			2870		This work
HREELS(111)	2840	2912					3,9
SFG(111)	2830						8,9
SERS(100)			2835	2865		2928	This work
HREELS(100)						2927	3,9
SFG(100)						2900	8,9
FTIR powder	2858	2952	2835	2935	2880		4
<i>Ab initio</i> MO calc. ^b							
$\nu \times 0.9^c$ (ν)	2853 (3170) ^d	2905 (3228) ^d	2844 (3161) ^e	2884 (3204) ^e	2868 (3187) ^f	2903 (3225) ν_{out}^g 2920 (3245) ν_{in}	This work

^aSym.: symmetric; deg.: degenerate; asym.: asymmetric; str.: stretching.

^bHartree Fock level with $6-31+G(d,p)$ basis set.

^cScaling factor, Refs. 16–18.

^dFigure 1(a).

^eFigure 1(c).

^fFigure 1(b).

^g ν_{out} : Two CH out-of-phase stretching modes of the H-C-C-H dimer portion; ν_{in} : Two CH in-phase stretching modes of the H-C-C-H dimer portion [Fig. 1(d)].

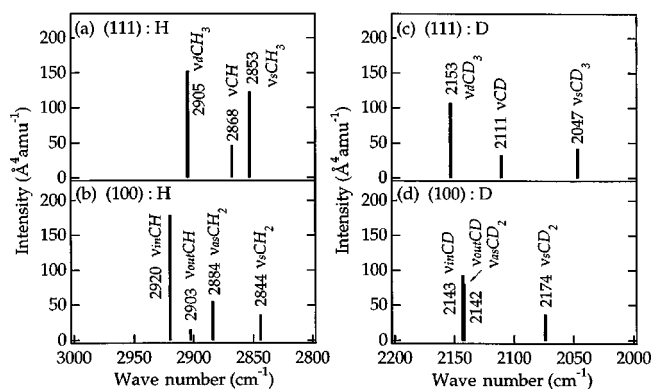


FIG. 4. Calculated Raman spectra for the diamond (111) and (100) surfaces by *ab initio* MO calculations. (a) Hydrogenated diamond (111) surface by using cluster (a) and (b) of Fig. 1. (b) Hydrogenated diamond (100) surface by using cluster (c) and (d) of Fig. 1. (c) Deuterated diamond (111) surface by using cluster (a) and (b) of Fig. 1. (d) Deuterated diamond (100) surface by using cluster (c) and (d) of Fig. 1.

and STM studies proposed a structure with dimer rows by monohydride termination for the (100)- 2×1 surface.³ A main peak at 2928 cm^{-1} was a dominant characteristic in the SERS spectrum [Fig. 3(I)], and a weak board shoulder tailed in the lower wave number region. The *ab initio* calculation results suggest that the main peak at 2928 cm^{-1} is due to the C-H stretching vibrations, and tailed peaks are due to CH_2 stretching vibrations as shown in Fig. 4(b). The main peak at 2928 cm^{-1} was assigned to the C-H in-phase stretchings. The *ab initio* calculations indicated that the C-H stretching should have two modes, one at 2920 and one at 2903 cm^{-1} . In principle, C-H monohydride species has only one mode for the stretching vibration. However, the diamond (100)- 2×1 surface has dimer rows, and they should have two stretching vibration modes. One is the in-phase stretching mode which is a symmetric stretching, and the other is the out-of-phase stretching mode which is an asymmetric stretching.

HREELS study has indicated that the hydrogenated diamond (100) surface was a terminated C-H monohydride species.³ HREELS has the highest resolution among electron spectroscopies, but the resolution is about 1–2 meV

($1 \text{ meV} = 8.066 \text{ cm}^{-1}$), which is less than those of Raman spectroscopy. The resolution of the HREELS also depends on the surface smoothness of the atomic order. For this reason, only HREELS spectra with 5-meV resolution have presented one peak of the C-H stretching vibration on the diamond (100) surface. SERS has a much higher resolution and could show two C-H stretching modes. Figure 3(b) also shows two peaks; one at 2830 cm^{-1} and one at 2865 cm^{-1} , which were assigned to the CH_2 symmetric and CH_2 asymmetric stretching vibrations. These peaks, due to CH_2 stretching vibrations, arose from the step edges, ledges, kinks, and disordering of the dimer rows and missing rows. The intensity ratio of the C-H peaks to the CH_2 peaks should suggest the degree of perfection achieved by the surface atomic structure.

The isotope shift was predicted by the *ab initio* calculation. Recently, Mantel and co-workers successfully observed C-D stretching vibrations on the diamond (100)- 2×1 surface using the FTIR attenuated total reflection (ATR) method.⁶ They presented C-D stretching at 2181 cm^{-1} . The present SERS indicates a main peak at 2195 cm^{-1} . The observed frequencies by FTIR-ATR and SERS are in good agreement. Although the prediction of the C-H stretching vibration frequencies by *ab initio* calculation are in good agreement with the experimental data, the calculated frequencies of C-D stretching vibrations tend to be lower than the experimental results of SERS.

SUMMARY

SERS spectra on the hydrogenated and deuterated diamond (111) and (100) were presented first. SERS peaks of C-H and C-D stretching vibrations were compared to vibrational spectroscopic results previously reported and to values assigned by *ab initio* MO calculations. The present results show that SERS has a potential advantage for demonstrating surface vibrations of small crystals, which are difficult to observe using other vibrational spectroscopies.

ACKNOWLEDGMENT

We would like to thank K. Watanabe for his assistance in Raman measurements.

*Author to whom correspondence should be addressed. Electronic address: ando@nirim.go.jp

¹S.-Tong Lee and G. Apai, Phys. Rev. B **48**, 2684 (1993).

²B. Sun *et al.*, Phys. Rev. B **47**, 9816 (1993).

³T. Aizawa *et al.*, Phys. Rev. B **48**, 18 348 (1993).

⁴T. Ando *et al.*, J. Chem. Soc., Faraday Trans. **89**, 1383 (1993).

⁵T. Ando *et al.*, Diamond Relat. Mater. **4**, 607 (1995).

⁶B. F. Mantel *et al.* (unpublished).

⁷R. P. Chin *et al.*, Phys. Rev. B **45**, 1522 (1992).

⁸T. Anzai *et al.*, J. Mol. Struct. **352/353**, 455 (1995).

⁹T. Ando *et al.*, *Advances in New Diamond Science and Technology* (MYU, Tokyo, 1994), p. 461.

¹⁰M. Fleischmann *et al.*, Chem. Phys. Lett. **26**, 163 (1974).

¹¹D. L. Jeanmaire and R. P. van Duyne, J. Electroanal. Chem. **84**, 1 (1977).

¹²R. Dornhaus *et al.*, Surf. Sci. **101**, 367 (1980).

¹³J. Giergiel *et al.*, Phys. Rev. B **33**, 5657 (1986).

¹⁴H. Ishida *et al.*, Appl. Spectrosc. **40**, 322 (1986).

¹⁵M. J. Frisch *et al.*, GAUSSIAN 98, Revision A.3, Gaussian Inc., Pittsburgh, PA, 1998.

¹⁶J. A. Pople *et al.*, Int. J. Quantum Chem., Quantum Chem. Symp. **15**, 269 (1981).

¹⁷J. A. Pople *et al.*, Isr. J. Chem. **33**, 345 (1993).

¹⁸T. Uchino and T. Yoko, J. Phys. Chem. B **102**, 8372 (1998).

¹⁹S. A. Solin and A. K. Ramdas, Phys. Rev. B **1**, 1687 (1970).